Ordering kinetics of a chemisorbed overlayer: O/W(110)

P. K. Wu,* M. C. Tringides,† and M. G. Lagally‡
University of Wisconsin–Madison, Madison, Wisconsin 53706
(Received 15 March 1988; revised manuscript received 29 November 1988)

The ordering kinetics of an oxygen submonolayer on W(110) is investigated at several coverages and temperatures using low-energy electron diffraction. Coverages correspond to ordering in a single-phase region and two different two-phase coexistence regions. The growth follows a power law at early times at each coverage. Dynamic scaling of the growth is investigated at two coverages. It is shown that from the activation energy for the ordering process, an activation energy for nonequilibrium diffusion can be determined. The values are compared to those for equilibrium diffusion.

I. INTRODUCTION

The kinetics of ordering or growth of two-dimensional (2D) systems has recently attracted considerable attention.[1–13] Of major interest has been the form of the growth law in different regions of the phase diagram, the influence of ground-state degeneracy, and the question of scaling in the growth. We report here a crystallographic determination, using low-energy electron diffraction (LEED), of the growth of domains in a two-dimensional disordered system that is suddenly forced to a condition where the thermodynamic-equilibrium state is an ordered superlattice. We address the questions of growth law and scaling at different coverages, at which the system exists in different phase regions. We show that the coverage dependence of the activation energy for diffusion of adsorbed species can be extracted from the measurements.

In this section we review relevant aspects of the system under investigation, O/W(110), including structure, degeneracy, and phase diagram, and summarize theoretical developments that are applicable to its ordering kinetics. Oxygen chemisorbed on W(110) is ideal for this study because it has been extensively investigated and forms several ordered structures at different coverages, which, because of their lower symmetry relative to the substrate, can form in several states that are degenerate in energy. For example, at room temperature, three structures, $p(2\times1)$, $p(2\times2)$, and $p(1\times1)$, corresponding to $\frac{1}{2}$, $\frac{3}{4}$, and 1 monolayer coverage, are observed. These may have, depending on the adsorption site, a degeneracy of at least four and as much as eight. There are four possible adsorption sites on the W(110) surface: on-top, short-bridge, threefold-hollow, and long-bridge. Four different degenerate $p(2\times1)$ structures, differing either rotationally or translationally, are possible for the long-bridge and on-top sites. There are two short-bridge sites per unit cell. Four different $p(2\times1)$ structures can form at each of these sites. A total of eight different $p(2\times1)$ structures can therefore be formed, which are not necessarily degenerate in energy because two types of bond configurations are involved. The degeneracy is thus equal to 4. If the oxygen sits on threefold-hollow sites there will, however, be eight degenerate states, because the two threefold-hollow sites in a unit mesh are entirely equivalent. Four translationally and four rotationally equivalent structures, shown in Fig. 1, can form. There is experimental evidence that $p=8$.[10]

For the $p(2\times2)$ structure, four degenerate states can form with all adsorption sites except for the threefold-hollow site, for which there are again eight possible degenerate structures.

A possible phase diagram for O/W(110) has been constructed from measurements of the appearance of superlattice reflections in LEED as a function of temperature at different coverages.[14,15] It is shown in Fig. 2(a). At room temperature and low coverages there is a first-order phase boundary separating a disordered lattice-gas phase from a coexistence region consisting of lattice gas and islands of oxygen atoms with a $p(2\times1)$ structure. For increasing coverages a single-phase region for the $p(2\times1)$ structure appears around $\Theta=0.5$. A single-phase region for the $p(2\times2)$ structure appears around $\Theta=0.75$. The

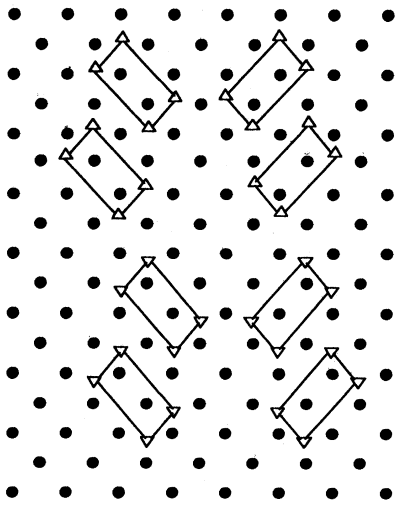

FIG. 1. Symmetry and ground-state degeneracy for W(110)$p(2\times1)$-O with occupation of the three-coordinated sites. The degeneracy is 8.

$p(2\times2)$ and $p(2\times1)$ phases may coexist at some intermediate range of coverages. For some coverage $\Theta > 0.75$ the $p(2\times2)$ structure coexists with the $p(1\times1)$ structure. Figure 2(a) also shows possible transitions to the disordered phase at high temperatures. The exact positions of most of the phase boundaries are not known. For example, the $p(2\times2)$ single-phase region can have a finite width instead of being a "line phase" as shown, and the $p(2\times1)$ phase can extend above $\Theta=0.5$. Similarly, the two-phase coexistence regions may have upper bounds that are somewhat lower than those shown. Transitions from the disordered to the $p(2\times1)$ phase are believed to be second order.[16,17] A calculated[18] phase diagram for this system is shown in Fig. 2(b). It is similar in the essential features, except that no coexistence region is indicated between the $p(2\times1)$ and $p(2\times2)$ phases, but rather a complex disordered phase.

If one considers a nonequilibrium phase transformation from the disordered state to an ordered state, one can expect that the approach to equilibrium depends on the nature of the final state. Various theoretical approaches to this problem have been made, and it is first necessary to establish which are applicable to the system at hand.[19] In O/W(110) the density is conserved, i.e., the number of oxygen atoms on the surface is fixed at the initially chosen coverage independent of the degree of order. Ordering cannot proceed by evaporation and condensation through the 3D phase, but must proceed by point-defect–vacancy exchange, i.e., by adatom hopping across the surface (or by more complicated 2D diffusional modes). Regions that have an excessive or deficient density of atoms relative to the ordered structure ("heavy" or "light" walls between adjoining domains) must attempt to achieve the mean by a diffusional mechanism—in many cases through particle exchange with already existing ordered regions.

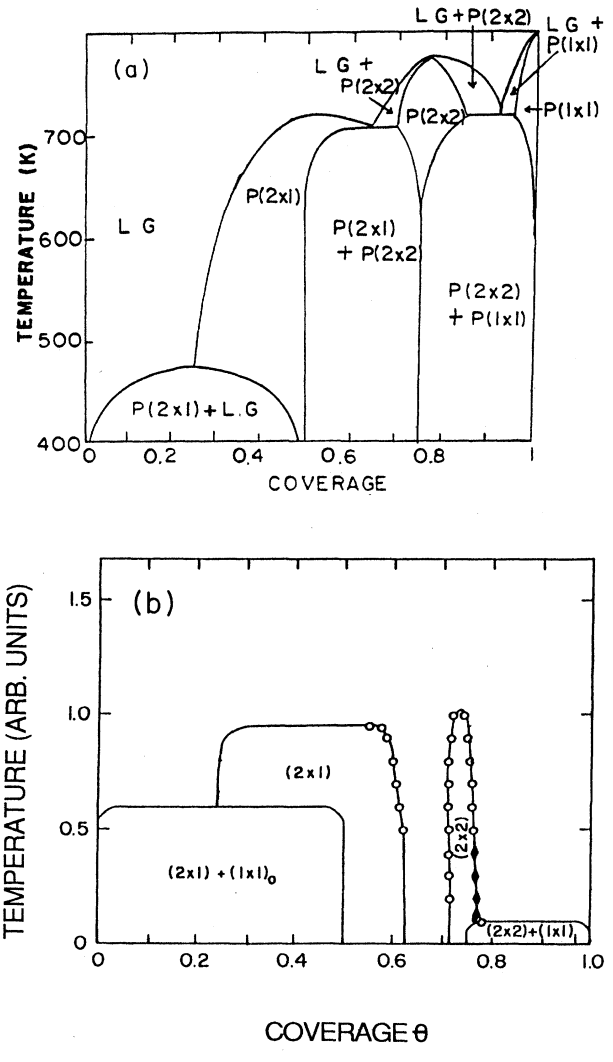

FIG. 2. Phase diagram for O/W(110). (a) Schematic diagram based on experimental measurements and the Gibbs phase rule. LG denotes lattice gas. (b) Theoretical, from Ref. 19.

The ground-state degeneracy p, which reflects the number and types of different domain walls, may also affect the ordering. As the overlayer symmetry relative to the substrate decreases [e.g., $(n\times m)$ layer], p increases. It seems physically reasonable that it becomes more difficult to order a layer as the number of types of domain walls increases. Early calculations showed a dependence of the growth kinetics on p. Recent calculations[20] on the Potts model indicate that the dependence may have been artificial. The influence of p on growth kinetics in other models appears to be a still unsettled question.[19(a),21] The nature of the final state (one-phase or two-phase coexistence) affects the ordering. As discussed below, the mechanisms for ordering that occur may be quite different.

Finally, ordering may consist of a sequence of competing processes that become important at different points in the time regime. A calculation may be relevant only for a specific range of the ordering process.

Most of the theoretical effort has concerned itself with the kinetics of ordering in a single-phase region of the phase diagram, beginning with the work of Lifshitz[1] for a two-dimensional system with ground-state degeneracy, $p=2$, and nonconserved density. A homogeneous disordered state that has been quenched into a one-phase region is allowed to order. This is shown schematically in Fig. 3(a). After initial domain formation the system will consist of many very small domains in contact, separated by walls. The continued domain growth is driven by a reduction in domain-boundary curvature (i.e., boundary free energy). The mechanism for domain growth appears to be interchange of particles with the 3D gas phase.[2–4] Lifshitz[1] found that the growth of domains driven by a reduction of boundary energy follows a power law,

$$\langle L(t)\rangle = A(T)t^{x}\,, \tag{1}$$

where $\langle L\rangle$ is the mean linear dimension of the domains, $A(T)$ is a temperature-dependent rate constant, t is time, and x is the growth exponent. For $p=2$ and nonconserved density all subsequent calculations[2–7] agree with Lifshitz's result that $x=\frac{1}{2}$ and that this exponent is universal, i.e., independent of the microscopic interactions of a particular system, as long as the degeneracy

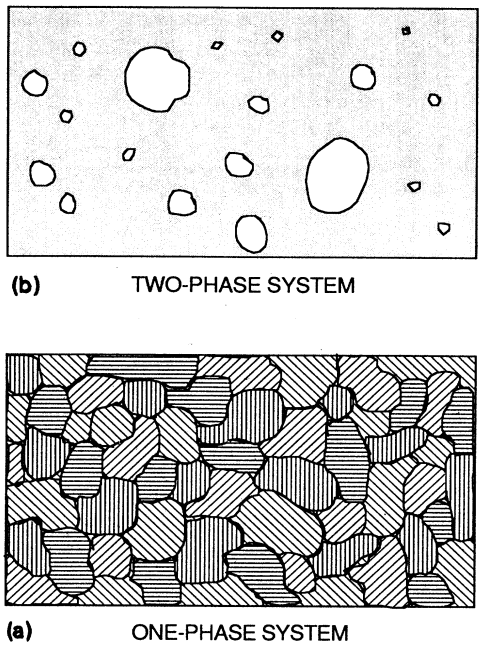

FIG. 3. Schematic diagram of the degree of order at some intermediate time for (a) a one-phase system with ground-state degeneracy $p=4$, and (b) for two phases coexisting with a low concentration of the dense phase. The dilute phase, consisting of monomers at lattice gas sites, is not explicitly shown.

$p=2$ is maintained. Calculations for larger values of p and nonconserved density[19,20] also generally produce an exponent $x=\frac{1}{2}$ for early stages of ordering. Thus, even though the dynamic and static critical exponents of models with, for example, $p=2$ and 4, are different (e.g., Ising model versus xy model with cubic anisotropy[16]), they yield the same domain-growth exponent. Lifshitz speculated that, for long times, the growth rate would slow down if $p>2$ because of polygonization, the formation of domains with straight boundaries that meet at vertices in such a manner that there is no driving force for further reducing boundary length.

In the system we have studied the above treatments may not be applicable. Domain growth at $\Theta=0.5$ in W(110)$p(2\times1)$-O corresponds to ordering in a single-phase region, but with conserved density. This situation has been treated in detail by Sadiq and Binder.[7] For a degeneracy $p=2$ it is again found that $x=\frac{1}{2}$, as for nonconserved density. For $p=4$ the calculations give $x=\frac{1}{3}$, lower than the corresponding value for nonconserved density, implying that the conservation of density is important in determining the universality class for $p>2$. It is reasoned that the growth is slowed by the lack of possibility of atom exchange with the gas phase, requiring long-range surface diffusion, and by the complexity of domain walls that can now exist.[7,19(a)] There is not, however, unanimity on this issue, as already mentioned. The degeneracy in W(110)$p(2\times1)$-O is at least 4, and possibly 8.[10] To our knowledge, no specific calculation has been made for conserved density and $p=8$. If $p=4$, the results of Ref. 7 are congeneric with the measurements at $\Theta=0.5$ that we present below.

Ordering when the coverage is low enough so that not all of the surface can be filled with ordered structure requires two-phase coexistence as the thermodynamic final state. A homogeneous disordered phase is quenched to a temperature at which a high-density phase [the $p(2\times1)$ structure] and a low-density one (the lattice-gas or 2D vapor phase) coexist. Immediately after the quench, the system will continue to exist as a low-density homogeneous disordered state (vapor phase), which at the low temperature represents a state of supersaturation, however, Nucleation of ordered islands takes place randomly. Figure 3(b) shows a two-phase system at this stage. All islands grow, by monomer addition from the vapor (effectively a 2D condensation), until the supersaturation is eliminated and the islands are in local equilibrium with their vapor. The simplest mechanism for island growth is long-range diffusion of monomers. After the mean supersaturation is reduced to zero, subsequent ordering of the system takes place by coarsening, in which small islands disappear at the expense of large ones. The process is driven by the difference in boundary free energy of islands of different size. The mechanism is 2D evaporation and/or condensation with long-range monomer diffusion. There is some difference of opinion in the literature in the use of the word "coarsening." In some cases, what we have termed "growth" from a solution with a mean supersaturation (all islands growing) is considered the "early stage" of coarsening. The "late stage" of coarsening is then the regime where small islands disappear at the expense of the larger ones. In other cases, "coarsening" is reserved for this late stage. We will use growth and coarsening to reflect the two regimes.

The classical theory of coarsening is that due to Lifshitz and Slyozov.[8] Their work is a mean-field kinetic theory for the size evolution of (1×1) islands of one phase (the dense phase) in a sea of the other (dilute lattice gas) phase, in the limit of vanishingly small density of (1×1) islands. The theory predicts a growth exponent of $x=\frac{1}{3}$. The growth mechanism involves 2D evaporation and/or condensation, and diffusion. There have been subsequent efforts to extend the theory[21–23] to finite densities of islands, which involve, as is physically necessary and apparent, interactions between the islands because they all contribute to the density of monomers in the dilute phase. There is agreement that $x=\frac{1}{3}$ independent of the density. The more complete theories[22] of kinetics of first-order transformations show, as we have already described above, two regimes: growth (changing mean supersaturation) and coarsening (constant total island volume, but reduction in boundary length). These theories to our knowledge all reflect the ordering of (1×1) islands coexisting with disordered lattice gas. In our case, the ordered regions exist as a superlattice. Because now antiphase boundaries are possible, the results mentioned above may not apply directly. Physically it seems as long as the density of islands is low, their antiphase relationship should have no bearing on the coarsening, because a simple evaporation and/or condensation mechanism can still be effective. Thus one would ex-

pect a growth exponent of $x=\frac{1}{3}$. If the density of ordered islands becomes high, they begin to meet occasionally at antiphase boundaries. One might expect at higher coverages a transition to the ordering kinetics in a single-phase region described earlier. If the growth exponent in both types of phase regions is $x=\frac{1}{3}$ for $p=4$, as predicted, one would not observe any change in x with coverage. For a system with $p=2$, one might, on the other hand, expect to see a transition from an exponent $x=\frac{1}{2}$ at saturation coverage (single-phase region) to an exponent $x=\frac{1}{3}$ at sufficiently low coverages in the two-phase coexistence region.

An aspect of theories for ordering in both the one-phase and coexistence regions is that they frequently exhibit dynamical scaling over a range of ordering times.[1-8] Scaling in the growth means that the size distribution function of ordered domains, $P(N,t)$, changes its mean value and width in such a manner that a specific scaling function,

$$P(N,t)=F(N(t)/\langle N(t)\rangle)\ , \tag{2}$$

can be defined, where $N(t)$ is the number of atoms in a domain at time t. Dynamic scaling implies self-similar growth: the distribution of domain sizes at one time can be related to that at another time by a simple magnification. Scaling appears to imply that only one ordering mechanism is active. Scaling is generally found for domain growth in a one-phase region, unless defects are present, which may act to destroy scaling. The Lifshitz-Slyozov theory for coarsening in a two-phase region also exhibits scaling. More thorough treatments[21,22] show that for early times in two-phase ordering, when a mean supersaturation still exists, scaling is not observed until this supersaturation is eliminated and the density of "solid" phase becomes a constant. The relationship of these results to the system under investigation will be discussed below.

II. EXPERIMENT

The experiment consists of measuring the LEED intensity from the overlayer as a function of time, at different temperatures and coverages. Intensity measurements are made with a diffractometer consisting of an electron gun, a two-circle goniometer, and a moveable Faraday cup with a circular aperture. Provisions are made for sample heating, cooling, temperature measurement, and oxygen and argon dosing. The chamber background pressure is in the high-10^{-11}-Torr range, with partial pressures of reactive contaminant gases, such as CO_2, CO, and H, in the low-10^{-11}-Torr range or lower. The angular distribution of intensity in a diffracted beam is measured by electrostatically scanning the incident beam across the sample so that the diffracted beam moves across the aperture of the Faraday cup, after first mechanically positioning the Faraday cup at the beam maximum. In this measurement the position of the beam on the sample changes, and it must be assumed that the surface structure and defect concentration are uniform over the area over which the beam sweeps. The current is measured with an electrometer or, alternatively, by imposing a small ac signal on the Wehnelt cylinder of the electron gun and monitoring the in-phase component of the diffracted current with a phase-lock amplifier.

Overlayer ordering experiments begin with an evaluation of the instrument resolving power and the defect structure of the substrate. An estimate of the instrument resolving power can be made from the full width at half maximum (FWHM) of the beam and the measurement accuracy. The FWHM of the (0,0) beam is constant at $\sim 1.1°$ down to ~ 80 eV, below which it increases. The variation of the FWHM's of angular profiles taken under identical experimental conditions is always less than 15%. The minimum angle of resolution[24] for our instrument is calculated to be 0.7° at 70 eV, which gives a maximum resolvable distance (MRD) of 65 substrate lattice constants (~ 180 Å). At 25 eV, the MRD is ~ 125 Å. The MRD determined for diffraction geometries corresponding to other beams is similar or greater. The instrument thus has low resolution in comparison to the state of the art. However, as will be demonstrated, it is quite sufficient for the ordering kinetics measurements reported here.

Because steps may act as diffusion barriers that isolate adsorbed atoms on a given terrace, leading to a collection of noncommunicating thermodynamic subsystems,[15] it is important to assure that the average substrate terrace size is much larger than the maximum average overlayer domain size that is observed in the experiment. If steps exist on the surface, the FWHM will oscillate as a function of energy. This oscillation is a result of the interference of waves scattered from terraces at different heights. We do not observe any oscillations, indicating that, within the detection limit, there are no steps on the W(110) surface. An estimate of the lower limit of the average terrace size, obtained by assigning all the uncertainty in the measurement of the FWHM of a substrate beam as a function of energy to step oscillations, gives 55 substrate lattice constants per terrace.

Impurities can significantly affect the ordering kinetics,[13,21(b),25-27] acting as pinning sites for boundaries and possibly as nucleation centers for small islands. Thus the cleanliness of the surface is an important consideration. The W(110) surface was cleaned in the usual manner,[28] which produces a surface free of contamination. Contamination builds up over time and consists mostly of CO and H. The amounts adsorbed after a given time can be measured by thermal-desorption mass spectrometry. The maximum amount of impurity gases adsorbed on the sample prior to dosing with oxygen is found to be less than 0.1% of a monolayer,[14] occurring generally in the early stages of an experiment. Most of this is hydrogen. With additional cycles of O dosing, the impurity concentration drops.

The source of oxygen is a silver permeation leak tube. An oxygen pressure of 1×10^{-5} Torr is built up in the tube by heating it for several hours. A leak valve and a molecular-beam tube for dosing the sample are used to control flow and to decrease exposure time, thus reducing the amount of O exposure of other parts of the system and lowering the pumping load. The equilibrium partial

pressure of oxygen, $P_0(t)$, in the chamber during dosing is $\sim 2\times 10^{-9}$ Torr and remains constant over a large number of experiments. $P_0(t)$ is monitored and the leak tube recharged as necessary. To determine and control the coverage, exposure curves coupled with sticking-coefficient measurements are used.[29] For a normalization point of coverage versus exposure, the intensity maximum of the $(0,\frac{1}{2})$ reflection from the oxygen overlayer for room-temperature exposure is usually taken to represent half-coverage[30]. The rest of the coverage scale is then determined using sticking-coefficient measurements.[29] If $S(\Theta,T)$ is the sticking coefficient of oxygen on W(110) at Θ and T, then the change of the coverage, $d\Theta(t)/dt$, at the surface is

$$\frac{d\Theta(T)}{dt}=CP_0(t)S(\Theta,T)$$

or (3)

$$\int \frac{d\Theta(T)}{S(\Theta,T)}=C\int P_0(t)dt\ ,$$

where C is a constant that takes into account that we do not know the absolute pressure of oxygen at the sample, but only $P_0(t)$. C is found by integrating $1/S(\Theta, 300\text{ K})$ to $\Theta=0.5$, and $P_0(t)$ to $t_{0.5}(300\text{ K})$.

At temperatures where the oxygen overlayer does not order, e.g., at 200 K, superlattice-beam-intensity–versus–exposure curves are not available and some other means of coverage measurement is needed. The exposure time to reach half-coverage at 200 K, $t_{0.5}(200\text{ K})$, is first estimated using $P_0(t)$, $S(\Theta, 200\text{ K})$,[29] and $C(300\text{ K})$ and then found precisely by annealing at 600 K samples exposed to O for times varying by incremental amounts from this estimated value. The exposure time that gives the narrowest profiles is chosen to correspond to $t_{0.5}(200$ K). The value of C is finally recalculated using $S(\Theta, 200$ K) and the now independently determined $t_{0.5}(200\text{ K})$. The difference between $C(200\text{ K})$ and $C(300\text{ K})$ is about 8%.

For $\Theta<0.4$ the absolute coverage can be determined easily because S is large and not rapidly varying with coverage. For $\Theta>0.5$ this is not an accurate method, because of the small sticking coefficient. However, a given coverage is easily reproducible, because the coverage change with exposure time is small. Considerable effort was made to determine $\Theta=0.5$ accurately. The uncertainty of the measurement of $\Theta=0.5$ favors values below rather than above this coverage.

To measure growth kinetics the sample is cooled to 200 K and then exposed to oxygen until the desired coverage is obtained. At 200 K the adsorbed overlayer does not form superlattice structures, as indicated by the lack of superlattice beams and by a high diffuse intensity, representative of a disordered overlayer. The sample is then rapidly heated to and held at a particular annealing (growth) temperature. The peak intensity of a superlattice beam and the sample temperature are measured as a function of time at 1-s intervals. The intensity generally shows variations of $\pm 15\%$ that are a consequence of electrometer drift at the very small currents ($\sim 10^{-13}$ A) that we are measuring. At specific times (100, 200, 300, 400, 500, 700, and 900 s) the sample is rapidly cooled, and the intensity distribution in a superlattice beam (angular profile) is measured. The temperature drop over the range of annealing temperatures used here is of the order of 30 K, enough to freeze the structure for the time to make an angular-profile measurement. The sample is then rapidly heated again to the annealing temperature and the experiment is continued. The temperature reaches the desired value in ~ 7 s, oscillates about this value for ~ 20 s, and thereafter remains within 2 K of this value. The time scale of these variations in temperature is thus small compared to the time scale important in the kinetics. We consider the annealing cycle to begin when the sample temperature is within 5 K of the annealing temperature and to end when the sample temperature is more than 5 K below the annealing temperature. All growth that occurs below $T-5$ K is ignored. The error introduced in the intensity caused by growth below $T-5$ K can be estimated using the measured activation energy (see below) and is of the order of 5–10 %, with the higher values corresponding to higher growth temperatures. In general, to prevent the interpretation of time-dependent variations in the experimental parameters as an aspect of growth kinetics, both the annealing temperature and the coverage for consecutive runs are chosen randomly. Such variations include adsorbed impurities (generally the system becomes cleaner for later runs; see above) and variations in oxygen pressure during dosing.

At the end of each experiment, the sample is annealed at ~ 500 K and the $p(2\times 1)$ structure is allowed to order at that temperature for a short time to reach its best structure. After cooling the sample to room temperature, the $(0,\frac{1}{2})$-beam profile is remeasured. The profile for the fully annealed structure should be the same for all experiments at the same coverage. The shapes of such profiles from different experiments are usually the same, but the peak intensity generally varies slightly, $\pm 15\%$, as a consequence of incident-electron-beam intensity fluctuations. We use the integrated intensity of $(0,\frac{1}{2})$-beam profiles from the fully annealed structure as a normalization factor in all analyses where comparison of the absolute intensity between different data sets is required. Data sets with very different profiles for fully annealed structures are discarded.

III. GROWTH LAW AND ISLAND SIZE AT $\Theta=0.5$

In this section we begin with a general discussion of the determination of the growth law of two-dimensional phases from measurements of the peak intensity of superlattice beams and the domain size from angular profiles. We then describe the results at $\Theta=0.5$.

A. Peak intensity measurement and growth law

Consider diffraction from a single two-dimensional domain with a superlattice and a linear dimension $L\sim N^{1/2}$. The peak intensity of a superlattice beam diffracted from the domain can be written in terms of N as

$$I_{\text{superlattice}}(s=0,\,t)=|f(\theta,E)|^2 N^2(t)\ , \tag{4}$$

where s is the deviation parameter from the Bragg condition and $f(\theta,E)$ is the atomic scattering factor of each atom in the domain. If there are P domains on the surface, each with N atoms, the total number of atoms on the surface is PN, and the peak intensity at any instant is

$$I_{\text{superlattice}}(0,\,t)=|f(\theta,E)|^2 PN^2(t)\ . \tag{5}$$

At constant coverage, to conserve the total number of atoms, PN must be constant and thus $P=C/N(t)$. The evolution of peak intensity with time is therefore proportional to $N(t)$, i.e.,

$$I_{\text{superlattice}}(0,T)=|f(\theta,E)|^2 CN(t)\ , \tag{6}$$

where C is a constant. This result depends on conservation of the number of scatterers and on the fact that the intensities from individual islands of an overlayer that forms a superlattice can be summed incoherently (see below).[31] For a system in which there is a distribution of island sizes, but which exhibits self-similar growth, it can easily be shown that $N(t)$ can be replaced by a constant times $\langle N(t)\rangle$.

Although a limited instrument response does not affect the above arguments, it will introduce uncertainties in the measurements. A finite-size detector cannot measure $I(0,t)$; instead it integrates the intensity around $I(0,t)$ within an area the size of the detector aperture. If the FWHM of the diffracted beam is large compared to the instrument response using a circular aperature, the measured peak intensity is a good approximation to $I(0,t)$. The instrument response function at the diffraction conditions of our experiments is 3 times narrower than the narrowest profile measured for any of the growth experiments. The difference between the measured value and the true peak intensity is estimated to be always less than 5%. The greatest error occurs at late times, as the true profile gets narrower and thus the instrument response becomes more important.

One can check for a power-law–growth time dependence for the domain size by plotting ln(intensity) versus ln(time). Combining Eqs. (1) and (6) gives

$$I_{\text{superlattice}}(0,t,T)\propto\langle N(t,T)\rangle\propto A^2(T)t^{2x}\ , \tag{7}$$

If there is a power-law time dependence, the data should fit a straight line with the slope of the line equal to $2x$. A typical example is shown in Fig. 4(a). Data taken at seven temperatures between 260 and 300 K and plotted in this manner give a mean value $2x=0.56\pm0.04$. Intensities for three of these temperatures are shown in Fig. 4(b) plotted versus (time)^{2x}. The normalization factor is the integrated intensity of the fully annealed profile. The slopes of the fits to the data in Fig. 4(b) are temperature dependent and proportional to $A^2(T)$. If one assumes that $A(T)$ has an Arrhenius-like temperature dependence, such that

$$A(T)=A_0\exp(-E_{\text{meas}}/k_BT)\ , \tag{8}$$

where E_{meas} is an activation energy, A_0 is a frequency factor, and k_B is Boltzmann's constant, one can extract E_{meas} for the ordering process. This is shown in Fig. 5. The activation energy for initial ordering at $\Theta=0.5$ is found to be 0.17 ± 0.03 eV. The relationship of E_{meas} to an activation energy for surface diffusion will be explored in Sec. VII.

B. Late-time behavior

As ordering proceeds, eventually a stage is reached at which the rate of increase of the intensity slows down. This is observed in our data, as well as the results of others.[7,13,19,21,25–27] There are several physically plausible causes. In a single-phase system, polygonization, the achievement of straight domain boundaries meeting at fixed angles, can slow the growth, even if the substrate is perfect and free of impurities.[1,32] In two-phase systems, in the final stage of Ostwald ripening, where all islands have reached about the same size, the growth must slow down. There are also extrinsic reasons why the growth may slow. For example, if growth of the overlayer occurs on a substrate with terraces, and the terraces are thermo-

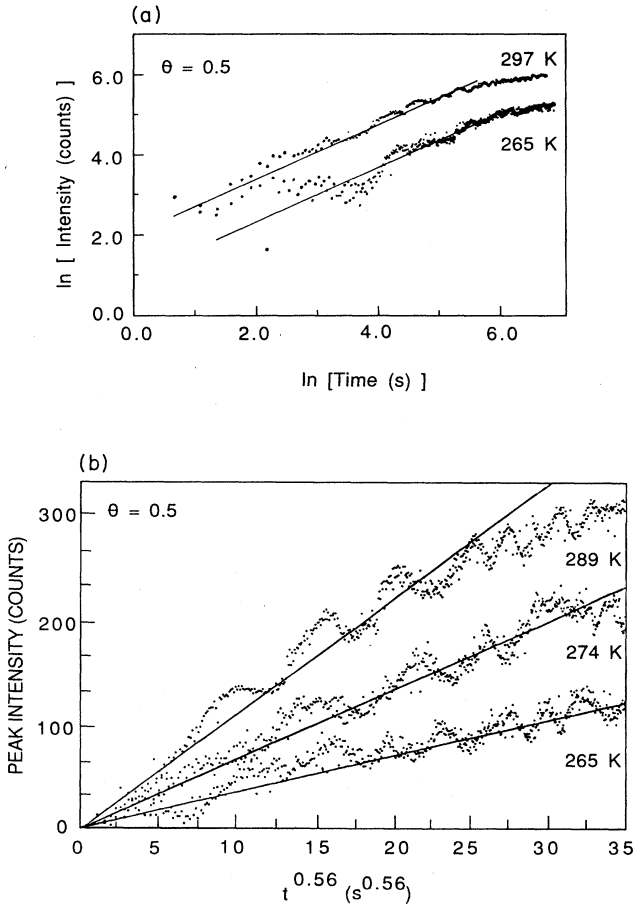

FIG. 4. Evolution of the peak intensity of a superlattice beam of $p(2\times1)$-O with time at $\Theta=0.5$. (a) ln$I$-vs-ln$t$ plot at two temperatures. (b) Peak intensities at three temperatures plotted vs (times)^{2x}, where $2x$ has been determined from plots such as those in (a). The "oscillations" in the data are noise that is a consequence of measuring very small currents.

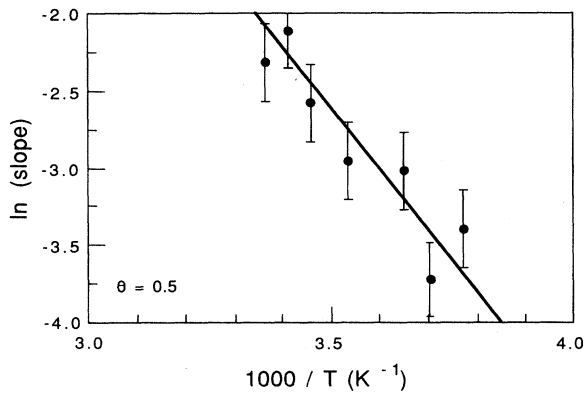

FIG. 5. Arrhenius plot of the slopes in Fig. 4(b). The fit to the data gives E_{meas}, the activation energy for the ordering process.

dynamically independent in the sense that mass transport across steps is very slow, then ordering can occur only within each terrace. There will be a limited supply of adatoms, and the domains or islands size may reach a limited size as a consequence. Additionally, point defects may slow the growth.[13,25–27] Finally, there is the influence of the instrument on the measurement of the peak intensity. A finite-size aperture integrates more and more of the profile as the profile becomes narrower at late times. As a consequence, the relationship expressed by Eqs. (6) and (7) changes. If the actual growth exponent is constant, the measured intensity will show a reduction of its rate of increase with time.

We observe at all coverages a reduction at late times of the intensity increase from the power-law value at earlier times. The effect can be seen for $\Theta=0.5$ in Fig. 4. Using Eq. (7), the growth exponent, after being constant over some initial time regime, decreases gradually to a new, lower value, which at $\Theta=0.5$ is $x=0.13\pm0.05$. The time at which this slowdown occurs is temperature dependent, being shorter for higher temperature. The intensity at which the growth slows down is also temperature dependent, with a higher value, corresponding to a larger value of $\langle N \rangle$, achieved at higher temperature. This behavior is inconsistent with impurity models of growth slowing.[27] Possible reasons for this behavior[14] will be briefly discussed in Sec. VIII.

C. Domain-size distribution

As growth proceeds, the sizes and size distributions of ordered domains change. The time evolution of the domain-size distribution function contains information on the growth mechanism and the rate-limiting steps in the growth kinetics. The size distribution can, in principle, be determined from angular profiles of the diffracted intensity in superlattice reflections. There are two orientations for $p(2\times1)$-O structures on W(110), i.e., $p(2\times1)$ and $p(1\times2)$. The kinematic structure factors of $p(2\times1)$ and $p(1\times2)$ domains are, respectively, zero at the positions of the superlattice beams of the other and thus one orientation does not contribute to the superlattice beam intensities of the other, but rather acts like empty space, or "sea," for the other. However, domains with the same orientation but with a translational antiphase relationship will contribute intensity at the respective superlattice reflections. As long as the positions of the antiphase boundaries are assumed to occur randomly, the interference between domains is small.[31] The superlattice beam intensities are then the sum of the intensities scattered from individual domains,

$$I(\mathbf{S},t)=\sum P(N,t)\frac{\sin^2 N(t)(\mathbf{S}\cdot\mathbf{a})/2}{\sin^2(\mathbf{S}\cdot\mathbf{a})/2}\ , \tag{9}$$

where $P(N,t)$ is again the probability of finding a domain with N atoms.

On any surface the size and separation distributions of the islands or domains are in actuality two-dimensional functions, and it is quite difficult to determine them. The conventional approach is to use one-dimensional models [as in Eq. (9)] and to project the actual two-dimensional distributions down to one dimension. This projection is done experimentally by using a slit detector or by integrating point detector measurements along one direction. The latter approach is used here. In separate papers[33] we will address the uncertainties in and limitations to using this approach. It can, in any case, be stated that mean island sizes determined from one-dimensional projections do not quantitatively represent the true sizes in the two-dimensional distribution. The distributions themselves become distributions of line segments. As a consequence, although we present actual values for mean sizes and size distributions here, they should be viewed as approximations.[33] However, because we use a consistent approach for all profiles, investigations of scaling in the growth should not be affected by the fact that we do not know the 2D distribution functions.

The influence of the instrument on the angular profile must be taken into consideration in order to determine the domain size distribution function from measured diffracted-intensity distributions. The instrument response function, independently measured, can be deconvoluted from the measured profiles. Alternatively, a distribution function $P(N)$ can be chosen and $I(\mathbf{S})$ calculated using Eq. (9). $I(\mathbf{S})$ is convoluted with the measured instrument function to obtain $J(\mathbf{S})$, which is compared with experimental profiles. Both methods were used here and gave consistent results. All profile measurements are made along the direction normal to a line connecting the (00), $(0,\frac{1}{2})$, and (0,1) reflections using a Faraday cup with a circular aperture small compared to the profile width. This line lies along the **a** direction in the primitive surface unit mesh, with $a=2.74$ Å.

Figure 6(a) shows a comparison of profiles at early and late times at $\Theta=0.5$. For all times and temperatures at which we were able to measure them, they are fitted best by a Gaussian domain-size (length) distribution [Fig. 6(b)]. A geometric size distribution also gives an approximate fit at early times, but gives wings that are increas-

ingly too high as the order increases. The Gaussian function has a FWHM corresponding to a length scale of approximately one overlayer lattice constant (which in this direction is the same as that of the substrate, $a=2.74$ Å). The maximum mean length measured within the range of annealing temperatures and times of the experiments (which corresponds here to the maximum mean separation between domain walls in the measurement direction) is a little more than five lattice constants. For comparison, the fully annealed structure gives a mean linear dimension of >40 overlayer lattice constants. The exact mean size and island-size distribution function are uncertain for the fully annealed structure because the diffracted-intensity profile from the fully annealed structure is instrument limited. This result indicates that, within the annealing time of our experiments, the system is far from ordering as completely as it could do, and contains considerable disorder. Measurements of profiles begin only after 100 s of ordering time have elapsed. A perusal of Fig. 4(a) shows that the turnover from the initial power-law–growth regime occurs at 400 s at the lowest anneal temperature (265 K) and at 200 s at the highest anneal temperatures (297 K). Hence essentially all of the profiles are measured in the regime in which the growth exponent determined from the evolution of the peak intensity is $x=0.13\pm0.05$. Averages of ln(inverse profile width)-versus-ln (time) plots at six temperatures give an exponent of $x=0.07\pm0.10$. The value is sufficiently uncertain so that it is not clear whether this represents agreement with the intensity data.

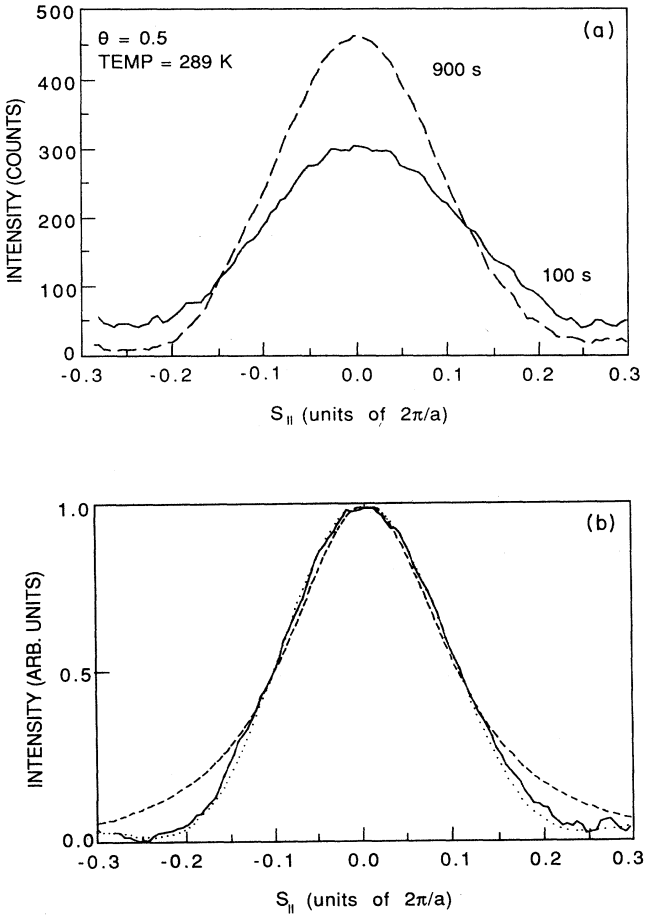

FIG. 6. Superlattice diffracted-beam profiles for W(110)$p(2\times1)$-O at $\Theta=0.5$. (a) Comparison of profiles at early and late times, indicating the profile shape and relative amounts of background; (b) fit to an angular profile (900 s at 289 K) using Gaussian ($\cdots$) and geometric ($-\ -\ -$) size distributions.

IV. GROWTH LAW AND ISLAND SIZE AT $\Theta=0.25$

At $\Theta=0.25$, the overlayer system is in a two-phase region in the phase diagram, with ordered O islands coexisting with lattice gas. Measurements of the peak intensity at this coverage show again a linear region on a ln$I$-versus-ln$t$ plot, with a changeover at long annealing times to a slower rate of intensity increase. The changeover occurs later in time than at $\Theta=0.5$ (>500 s at the highest temperature and later at lower temperatures), indicating that the initial ordering mechanism that we observe is maintained for a longer-time period. Angular profiles are again measured as 100, 200, 300, 400, 500, 700, and 900 s of annealing time. They are more complex than those at $\Theta=0.5$ and must be discussed somewhat more fully before one can have confidence in the interpretation of the intensity in terms of a growth law.

A. Island-size distribution

The discussion on the determination of the size distribution of domains presented above [Eq. (9)] holds as well for islands that are spatially separated. The island-size distribution function is found by fitting the $(0,\frac{1}{2})$ profile as described above. The measured profiles at $\Theta=0.25$ have a lower intensity and higher background. Both results are reasonable. There are fewer atoms scattering at $\Theta=0.25$, and more of them are in the disordered phase as a random lattice gas, or exist as very small islands. We determine the island-size distribution function as above by deconvoluting the instrument function, and choosing model size distribution functions to fit the resulting profile. Again, we use 1D models and thus really determine a projected length distribution function.[33] Profiles at all temperatures and times can be fitted well with two Gaussians, corresponding to islands with a bimodal size (length) distribution. Over the time scale and temperature range of the experiment the large islands range in mean size from ~3 to 9 lattice constants (in the measurement direction), somewhat larger than the maximum mean size at $\Theta=0.5$, and the small ones from ~1.5 to 3 lattice constants. The density of the small ones is about 3 times that of the large ones. These values are to a slight degree dependent on the fitting—mean size and concentration are somewhat cross-correlated in the model. We have not been able to fit the profiles with a single size distribution, but this does not imply that one does not exist. For example, an Ostwald ripening distribution function does have a tailing toward smaller sizes, but there appear

to be too many small islands in our data. We have no good physical interpretation for a bimodal size distribution.

B. Peak intensity measurement and growth law

For any complex island or domain-size distribution function the evolution of the peak intensity with time must be considered with caution. If the growth obeys scaling, i.e., if all the islands grow while the size distribution maintains its same functional form, then the peak intensity is still a good quantity to evaluate the growth law[34] and Eq. (7) applies to the entire island distribution. If the growth does not obey scaling, e.g., if a part of the size distribution evolves in a manner different from another part, then evolution of the peak intensity is not a valid measure of the growth law of the total system. It may still approximately reflect the growth law of part of the system, however. Consider a bimodal distribution of large and small sizes. The evolution of the peak intensity proceeds as $\langle N(t) \rangle$ [Eq. (6)]. If the concentration of large domains dominates, then the time dependence of the peak intensity of the diffracted beams from this structure will reflect approximately the growth of the large sizes, and Eq. (7) would approximately apply to this component. At other conditions, the development of the peak intensity becomes more complex.

In Sec. VI we will demonstrate that the angular profiles at $\Theta=0.25$ scale. Although we do not presently understand this scaling behavior, its existence implies that, independent of the identification of the correct size distribution function, the evolution of the peak intensity with time can be used to determine the growth law, Eq. (7).

Peak intensity measurements were made at six annealing temperatures in the range $265 < T < 300$ K. Figure 7 shows the results at three of these. The average growth exponent is found to be $x \simeq 0.28 \pm 0.02$. The activation energy for the ordering process, determined from the temperature dependence of the slopes of the curves in Fig. 7, is 0.16 ± 0.04 eV.

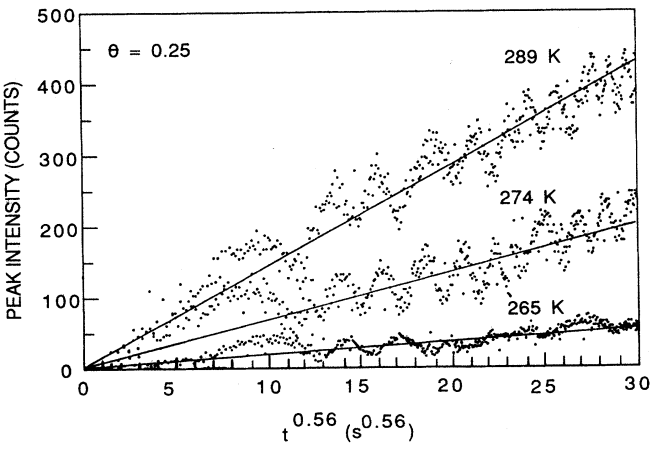

FIG. 7. Evolution of the peak intensity of a $p(2\times1)$ superlattice beam at $\Theta=0.25$ for several temperatures, plotted vs (time)^{2x}, where $2x$ is determined from ln$I$-vs-ln$t$ plots as in Fig. 4(a).

V. GROWTH LAW AND ISLAND SIZE AT $\Theta=0.65$

At $\Theta=0.65$, beams corresponding to the $p(2\times2)$ structure are observed. The system is probably in the region of coexistence (see Fig. 2) between the $p(2\times1)$ and $p(2\times2)$ structures. It cannot be definitively excluded that the system is in the $p(2\times2)$ one-phase region, because the superlattice beams that belong to the $p(2\times1)$ structure are also part of the $p(2\times2)$ structure, but it can be excluded that the system is still in the $p(2\times1)$ single-phase region. If an overlayer phase diagram of the nature of Fig. 2(a) is accepted, then at equilibrium at $\Theta=0.65$, by the lever rule, about half of the surface is covered with $p(2\times1)$ phase and the other half with $p(2\times2)$ phase.

The two-phase region at this coverage is different from the two-phase region at $\Theta=0.25$ in that the second phase is not a disordered lattice gas but rather an ordered structure with at least four degenerate states. The combined higher number of degenerate states creates more types of walls and one may expect[19(a)] the growth process to be slower than growth when one phase is a disordered lattice gas. For a system whose composition is in the center of the coexistence region, both phases will, to first order, have an equal probability of nucleating and will form in close proximity to each other. The diffusional path for monomers for one phase will need to cross the other ordered phase, slowing the growth process.

A. Island-size distribution

Data were taken at $\Theta=0.65$ for annealing temperatures in the range at $270 < T < 350$ K and times up to 900 s. Contrary to the results at lower coverages, there is no ordering observable below 300 K. This result implies that ordering is more difficult at $\Theta=0.65$ than it is at $\Theta=0.5$ and 0.25. Five data sets were taken between 300 and 350 K for the $(0,\frac{1}{2})$ beam. The measured intensity profiles are again fitted very well with a Gaussian size distribution function. The maximum size in the range of annealing temperatures and times of the experiment is less than seven overlayer lattice constants (mean domain size is less than 20 Å). The fully annealed structure gives a diffracted-intensity profile that is instrument limited (mean size > 120 Å). This indicates that, as before, the system has ordered only very little in the time and temperature regime we have considered.

B. Peak intensity measurement and growth law

The peak intensity follows a straight line on a ln$I$-versus-ln$t$ plot at early times and then changes over to slower growth at later times, as it did at the other coverages. The changeover occurs for $t > 300$ s at the highest temperatures, and at later times at the lower temperatures. The peak intensity has again been used to determine the growth law. The growth of domains [both $p(2\times1)$ and $p(2\times2)$, because both contribute to the $(0,\frac{1}{2})$ beam] fits a power-law time dependence. The growth exponent is found to be $x=0.20\pm0.03$. From the slopes of such intensity evolution curves with time [simi-

lar to those in Figs. 4(b) and 7] taken at five temperatures, the activation energy for the ordering process is found to be 0.13 ± 0.04 eV.

VI. SCALING IN THE ORDERING KINETICS OF O/W(110)

If an ordered structure grows in a self-similar fashion, the morphology of the system at any time is indistinguishable from that at an earlier or later time except for the magnification of the system. In this section we investigate scaling in the growth kinetics of W(110)$p(2\times1)$-O at $\Theta=0.25$ and 0.5.

The diffracted-intensity distribution, which is a measure of the degree of order of the system, changes with time during annealing. If the growth morphology is self-similar, the structure of the system, and hence also the diffracted-intensity distribution from the system, should be time independent except for a scale length, see Eq. (2). This result can also be expressed in terms of a "scaling function," $F(y)$, for the diffracted intensity, where $y=S/w(t)$ is a length in reciprocal space normalized to the FWHM, $w(t)$, of the profile measured at time t and where S is the magnitude of the momentum transfer. Then

$$F(y)=F(S/w(t))=\frac{I(S/w(t))}{I(0,t)}\ , \tag{10}$$

where $I(0,t)$ is the peak intensity of the profile at time t. If the system scales, then $F(y)=$const.

In order to test for scaling, it is convenient to remove the instrument response function from the measured profiles before they are compared. Alternatively, one could fit the profiles measured at different times with model profiles convoluted with the instrument response function and then check for scaling in the model profiles. We choose the first approach here. The profiles show a weak asymmetry that depends on the degree of order. The asymmetry becomes less noticeable the greater the order and hence the greater the intensity of the profiles. An asymmetry about $S_{\parallel}=0$ cannot be caused by any phenomenon related to island or domain size: all size or shape distributions will produce symmetric profiles. We conclude that, in all likelihood, the asymmetry is an artifact of the way the profiles are measured. Another, very speculative, possibility is the existence of domain walls caused by the possible occupation of the two "hourglass" sites in the unit mesh.[33(a)] Because we believe that the asymmetry is a measurement artifact, we have fitted only one-half of the profile and have reflected it about the peak to give symmetric profiles. A more detailed discussion appears elsewhere.[33(a)]

Starting with measured profiles, we obtain, using the convolution theorem, the properties of Fourier transforms, and a fast-Fourier transform routine, $I(\mathbf{S},t)$ from the measured profiles $J(\mathbf{S},t)$. $I(\mathbf{S},t)$ is then rescaled according to Eq. (10) above. Figure 8 shows profile scaling at two temperatures at $\Theta=0.5$. At the high temperature, all but the 100-s profile are measured in the time regime in which the peak intensity has slowed and thus the good overlap of the profiles indicate that there is dynamic scaling in the late-time domain growth. The profiles can be fitted with Gaussian functions, indicating that the size distribution of domains is also Gaussian. At the low temperature, the profiles are measured basically in the region of transition in which the evolution of the peak intensity [Fig. 4(b)] changes its slope. One would not expect scaling to be observed, and the profiles overlap much more poorly. We unfortunately cannot measure profiles rapidly enough to investigate scaling at $\Theta=0.5$ in the early-time regime in which we observe good power-law growth from the peak intensities.

Scaling of intensity profiles taken at $\Theta=0.25$ for different times at two temperatures is shown in Fig. 9. The deconvoluted profiles for $\Theta=0.25$ have greater intensity in the wings than are obtained for a Gaussian shape, but it appears that they still scale, to the accuracy of the experiment, with a single scaling parameter. The profile measurements here are primarily in the time regime before the peak intensity begins to slow its increase (see Fig. 7). This is so because this regime lasts longer at $\Theta=0.25$, as we have already pointed out, and is more

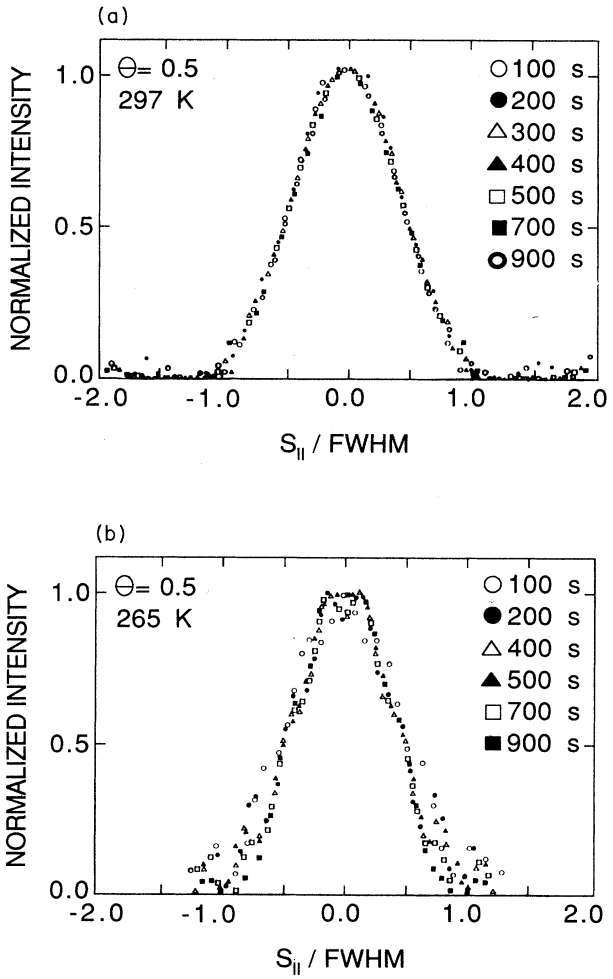

FIG. 8. Dynamic scaling in the growth at $\Theta=0.5$ at two temperatures. At 297 K, (a), the measurement times are in the late-time regime, see Fig. 4(a). At 265 K, (b), the measurement times are in the transition region.

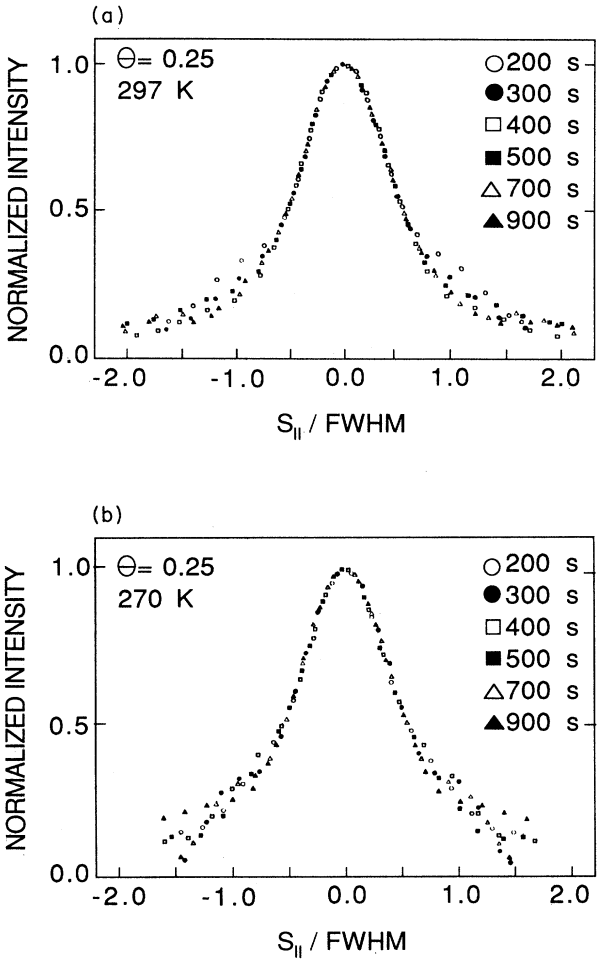

FIG. 9. Dynamic scaling in the growth at $\Theta=0.25$ at two temperatures. (a) 297 K, (b) 270 K. Profiles at both temperatures exhibit high wings, but about the same degree of agreement between profiles. Measurement times for the profiles correspond largely to the power-law region shown in Fig. 7.

true at lower than at higher annealing temperatures. The overlap of the profiles, if anything, is better at the lower temperature. We can fit the resulting profiles with a sum of two Gaussians, corresponding to a bimodal size distribution of two narrow Gaussians. It is more difficult to imagine physically that a bimodal distribution would exhibit dynamic scaling, and in all likelihood the profiles can be described also by a single distribution.

Although we did not make the same detailed analysis of the profiles at $\Theta=0.65$, scaling is indicated here as well. The profiles are Gaussians at all times and temperatures that we have been able to measure, and change widths in a continuous manner.

VII. DETERMINATION OF NONEQUILIBRIUM DIFFUSION COEFFICIENTS FROM ORDERING KINETICS MEASUREMENTS

The thermodynamic behavior of an overlayer is determined by the microscopic interactions between the adsorbate atoms and between adsorbate and substrate atoms. A determination of these microscopic interactions can be made at equilibrium or also as the system evolves toward equilibrium. The usual equilibrium measurement is the temperature-coverage phase diagram of the overlayer, made, for example, with a diffraction or specific-heat experiment. Using a statistical model with a few local interaction parameters and an underlying lattice geometry, the phase boundaries are fitted to find the magnitude of these interaction parameters. Nonequilibrium determinations of the same interactions can also be made, from measurements such as those reported here. The evolution of the system toward its equilibrium state requires mass transport. The temperature and coverage dependence of the ordering that we have discussed in this paper provides information on the microscopic interactions that govern nonequilibrium diffusion in the system.

It is to be noted that this diffusion is termed "nonequilibrium" to distinguish it from equilibrium diffusion. The simplest form of equilibrium diffusion that one can imagine is the random walk of a single particle among lattice-gas sites, for which the activation energy for diffusion is simply the corrugation of the substrate potential. For an overlayer, equilibrium diffusion is the random motion of atoms about their equilibrium sites. Measurements of such equilibrium diffusion have been performed by Gomer *et al.*[35] The activation energy for diffusion here depends on the interaction energies an adatom sees when it is in an equilibrium environment of neighbors. At temperatures and coverages at which the overlayer is ordered, the activation energy for diffusion will be high. At temperatures and coverages at which the equilibrium state is disorder, the activation energy will be lower, as the atom "sees" only a mean barrier due to the presence of random neighbors. It approaches the value for single-particle diffusion as the coverage approaches zero.

The factor $A(T)$ written in terms of an Arrhenius relationship in Eq. (8), contains the nonequilibrium diffusion coefficient, D. Theoretical determinations of the growth in both single-phase[2] and two-phase coexistence regions[8] have found that

$$A(T) \propto D^x , \tag{11}$$

where x is the growth exponent in Eq. (1). This relationship can be generalized on the basis of dimensional arguments to any growth situation (different ground-state degeneracies, etc.) with the assumption that the only time dependence on the right-hand side (rhs) of Eq. (1) occurs in D and in t^x. There are (as in Refs. 2 and 8) other constants (e.g., boundary energy, molar volumes, etc.) in Eq. (11), but they do not depend on time. The activation energy E_{meas}, in Eq. (8), obtained from a plot of $\ln A(T)$ versus $1/T$, can then be related to the activation energy for nonequilibrium diffusion, E'_{diff}, by

$$E_{\text{meas}}(\Theta)=xE'_{\text{diff}}(\Theta) . \tag{12}$$

From the values of x and $E_{\text{meas}}(\Theta)$ at three coverages, we deduce that the activation energy for diffusion of O on W(110) in a random environment of other O atoms lies in

the neighborhood of 0.6 eV/atom.

We would like to relate this value to the adatom interaction energies for $p(2\times1)$-O on W(110) found from fits to the phase diagram[36] and to equilibrium diffusion measurements[35] in this system. The phase diagram has been shown in Fig. 2(a), and a part of it is reproduced in Fig. 10(a). Monte Carlo fits to the phase boundaries require [see inset, Fig. 10(b)] a nearest-neighbor attraction ϕ_1, a next-nearest-neighbor repulsion ϕ_2, with $|\phi_1|\simeq|\phi_2|$, and a weaker third-neighbor attraction $\phi_3\simeq\phi_1/3$. Measurements of equilibrium diffusion[35] have been made over a coverage and temperature range [Fig. 10(a)] that includes the one-phase region and a disordered lattice-gas phase. The activation energy for equilibrium diffusion deduced from these measurements is shown as a function of coverage in Fig. 10(b). It shows a strong coverage dependence, as suggested earlier. The rise in activation energy occurs at the coverage at which the system orders. The magnitude of the rise is consistent with the interaction energies determined from the phase-diagram fits.[35] The value at lowest coverage, $E_{\rm diff}(\Theta=0.15)=0.6$ eV, represents an upper limit of the activation energy, $E_{\rm diff}(0)$, for single-particle diffusion. It is an upper limit because, even though the system is in a disordered phase, fluctuations can still create momentary ordered regions that will raise the activation energy.

Values of the activation energy $E'_{\rm diff}$ from ordering kinetics measurements, using Eq. (12) and the experimentally determined growth exponent x, are also shown in Fig. 10(b). These values can be related to the adatom interactions as follows. The value $E'_{\rm diff}$ represents the activation energy for diffusion for an atom in a mean environment. The mean environment of a diffusing atom is disorder—the random occupation of sites at the appropriate coverage. This can be expressed to first order as

$$E'_{\rm diff}(\Theta)=E_{\rm diff}(0)+Z\Theta\left[\sum\phi\right], \tag{13}$$

where Z is the coordination number of the lattice, Θ is the coverage, and

$$\sum\phi=\phi_1+\phi_2+\phi_3 \tag{14}$$

is the sum of the adatom-interaction energies. The second term in Eq. (13) thus represents the increase in activation barrier above the single-particle value caused by the presence of a randomly arranged set of neighbors. An atom in position 1 in the inset would contribute $-\phi_1$; in 2, $+\phi_2$; in 3, $-\phi_3$. This second term depends on coverage: the greater the coverage, the more occupied nearest-neighbor sites an atom is likely to have. The dashed curve in Fig. 10(b) is a plot of the coverage dependence of the activation energy $E'_{\rm diff}(\Theta)$, normalized to the value at $\Theta=0.25$. Its intercept at $\Theta=0$ gives the activation energy for single-particle diffusion.

Unfortunately, in this system, the influence of the mean adatom-interaction potential, $\sum\phi$, is rather weak (i.e., $\sum\phi\simeq0$), so to first order all of our measurements reflect the activation energy for single-particle diffusion, and only weakly a coverage dependence. We do not suggest, therefore, that our data are precise enough to deduce the dashed curve, but the methodology for determining the coverage dependence of the nonequilibrium diffusion coefficient is inherent in the results we have presented. If measurements of ordering are made at a variety of coverages, both $\sum\phi$ and $E_{\rm diff}(0)$ are, in princi-

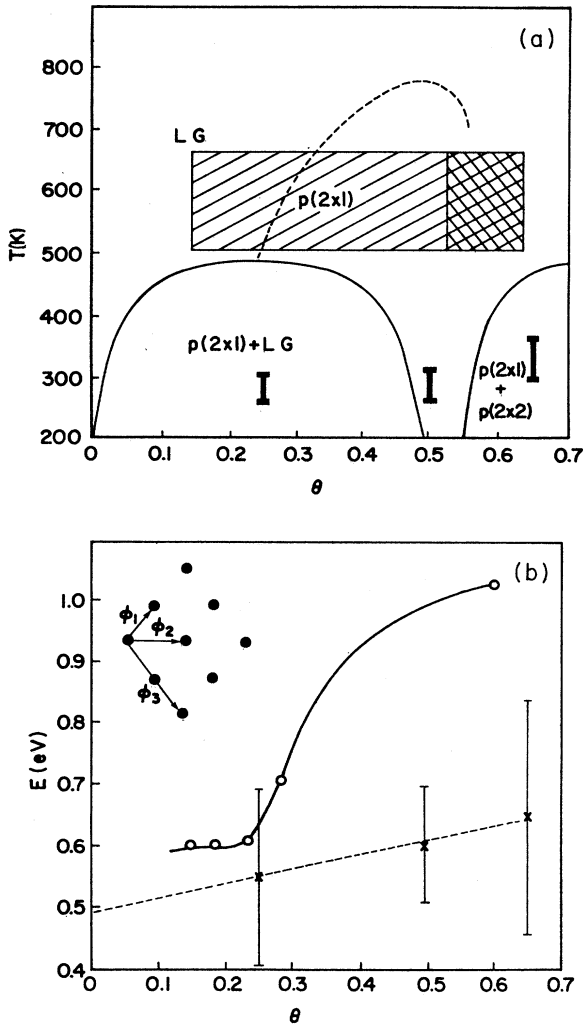

FIG. 10. Comparison of the equilibrium and nonequilibrium measurements of activation energies for diffusion of O on W(110). (a) Equilibrium phase diagram. The phase boundaries above $\Theta=0.5$ are uncertain. LG denotes lattice gas. The hatched region indicates the T-Θ range for equilibrium measurements (Ref. 35). The cross-hatching indicates a region where these measurements overlap the uncertain phase diagram. Heavy bars indicate T-Θ regions of the ordering kinetics measurements. (b) Activation energy for diffusion. Open circles: equilibrium measurements. Crosses: nonequilibrium measurements. The dashed line shows the coverage dependence of Eq. (12) using the interactions ϕ_1,ϕ_2,ϕ_3 shown in the inset. Their magnitudes (Ref. 36), determined from a best fit to the phase boundaries shown in (a), are -0.09, $+0.075$, and -0.03 eV. The curve is forced to go through the data point at $\Theta=0.25$. The intercept at $\Theta=0$ gives the activation energy for single-particle diffusion.

ple, extractable.

We also come to conclusions about the diffusional activation energy that are consistent with the equilibrium measurements of Gomer.[35] In phase regions where the equilibrium state is disorder, the determinations for the activation energy for diffusion are very similar to ours, which always reflects disorder, except for a coverage dependence. In regions where the equilibrium state is order, the activation energy for equilibrium diffusion is higher than $E'_{\rm diff}$ by an amount that is related to the adatom-interaction potential as seen by atoms in the ordered state.[35]

There are several assumptions in this analysis. One is that the arrangement of overlayer atoms is random. True randomness occurs only at zero time. In general, the system is more ordered, which increases the activation energy. In our measurements, the mean domain sizes change from ~ 2.5 atoms wide at early times to ~ 7 atoms wide at the latest times, and thus there is considerable disorder over the complete time regime. A second assumption is that the coverage is known. It can occur that the effective coverage for a diffusing species is lower than the mean coverage. e.g., in a two-phase system at a low degree of supersaturation. This latter effect is only important if $\sum\phi \neq 0$, and then generally it lowers $E'_{\rm diff}$. Because $\sum\phi \simeq 0$ here, our values should be reliable. A more accurate analysis will require weighting of each configuration with the proper probability factor and the use of Monte Carlo methods. A third assumption is that there are no extrinsic barriers to diffusion. There is always the possibility that impurities or defects affect the growth. They would tend to increase the activation energy, in the sense that they act as nucleation sites or sites blocking diffusion, implying that any measurements such as those described here give an upper limit to the activation energy for single-particle diffusion. The fact that our results give a consistent picture with equilibrium diffusion values from field-emission measurements that by their nature are very clean suggests that impurities play a negligible role in our experiments.

There are also other determinations[37,38] of the diffusion coefficient of O/W(110), using measurements of the evolution of an initial concentration profile with time. They are made at temperatures above the highest ordering temperature in the phase diagram, and thus are always representative of diffusion in a disordered system. They should therefore be comparable to our measurements and are, at least in their behavior. A slight coverage dependence is even indicated in one measurement.[38] However, both obtain values of activation energies that are too high relative to our measurements. We do not understand the difference. Concentration-profile–evolution measurements are much less microscopic than ours. We speculate that additional diffusion barriers, such as steps, act to raise the activation energy.

VIII. DISCUSSION AND CONCLUSIONS

In this paper we have presented measurements of the ordering kinetics of a submonolayer of O/W(110), in which the ground-state degeneracy is at least 4 and possibly 8. Measurements are made at different coverages, at which the system exists either as a single ordered phase or coexist with a second phase that is either a disordered lattice gas or a second ordered phase.

Measurements are made using diffraction. Both the peak intensity of superlattice reflections and their angular distribution of intensity are evaluated to determine the evolution of the mean domain size and the size distribution. One-dimesional models are used to fit the profiles and thus to determine the size distribution. From a comparison of profiles at different times but the same temperature, dynamical scaling in the growth is demonstrated in certain time regimes.

The evolution of peak intensity with time is used to determine growth laws in the different phase regions. A power-law growth is found at all three coverages that were investigated. In two of them [single $p(2\times1)$ phase and coexistence between $p(2\times1)$ and disordered lattice-gas phases], the growth exponent is found to be very similar, $x \simeq 0.28$. In the third [$p(2\times1)+p(2\times2)$ phase coexistence], the growth exponent is lower, $x=0.2$. Although much has been done, the state of the theory is not yet very advanced. Most effort has been expended in studying the growth dynamics with nonconserved order parameter, i.e., corresponding here to domain growth in the $p(2\times1)$ single phase. There are suggestions,[7] although not general agreement,[21] that $x \simeq 0.33$ for a system analogous to ours with $p=4$. We believe that actually[10,14] $p=8$, which may act to lower the growth exponent. The growth temperature may also influence the result.[7,19(a)] Our growth temperatures were of the order of $0.4T_c$ at this coverage. Most of the rest of existing calculations for single-phase ordering do not appear to be directly applicable to our system. They are applicable either to nonconserved density or for systems for which $p=2$, in which case there is general agreement that $x=\frac{1}{2}$.

For ordering in a two-phase coexistence region (conserved order parameter) there is general agreement that $x=0.33$ (Ref. 8) for the coarsening of the dense phase, independent of its concentration.[21(a),23] We find $x=0.28$. No theory exists, to our knowledge, specifically for coarsening of a phase that has a high ground-state degeneracy. At very low densities this should not matter. Our measurements are at $\Theta=0.25$, where equal concentrations of disordered lattice gas and $p(2\times1)$ phase coexist. The growth morphology (see Ref. 23) in all likelihood consists of interconnected domains. Such a growth in a two-phase coexistence region with high ground-state degeneracy may mimic single-phase growth with high degeneracy. Unfortunately, it is as yet unclear whether the exponent should be $\frac{1}{3}$ or $\frac{1}{2}$ in the single-phase region. If it is $\frac{1}{3}$, then the exponents are the same in both phase regions and it is not possible to address the question of evolution from and growth to another with coverage. In a $p=2$ system such an analysis should be possible, because the predicted exponent changes from $x=\frac{1}{2}$ to $x=\frac{1}{3}$ going from single-phase ordering to two-phase ordering. The growth temperature in this region is $\sim 0.6T_c$, higher than that at $\Theta=0.5$.

In two-phase coexistence, the sequence of growth of

domains of the dense phase from a supersaturated 2D vapor following nucleation is (1) growth of the dense phase to reduce supersaturation, and (2) coarsening driven by boundary-energy reduction. It is not likely that one growth law can describe both of these regimes. If one accepts that the intensity measurements shown in Fig. 7 correspond to the coarsening regime, it implies that supersaturation is eliminated very quickly. If, on the other hand, the time regime following the slowing of the increase of the intensity in Fig. 7 is assumed to correspond to coarsening, then the region at shorter times showing power-law behavior would be ascribed to growth to eliminate supersaturation. A power-law behavior in this region is inconsistent with theoretical conclusions.[22] It thus would appear that the slowing down of growth at late times is a phenomenon analogous to that observed at $\Theta=0.5$ and discussed in Sec. III B and below.

At $\Theta=0.65$, where two ordered phases coexist, we measure a distinctly lower growth exponent. The ordering should again be representable by a coarsening model. We do not know the respective concentrations of the ordered phases, but the most simple-minded guess, based on a lack of solubility of each phase in the other (i.e., the assumption that the single-phase region cuts off sharply at $\Theta\simeq 0.5$ and 0.75, respectively), would make the concentrations about equal, similar to the $\Theta\simeq 0.25$ coexistence region. Growth then likely again consists of connected regions with neither phase acting as the distinct matrix phase. A smaller exponent implies initially more rapid growth and a subsequently slower growth. The growth temperature is $\sim 0.45T_c$. Below $0.4T_c$ no ordering was observable in laboratory times.

It is worthwhile at this stage to summarize and discuss the overall growth behavior based on peak intensity measurements. If one measures with a true point detector, Eqs. (6) and (7) are correct for the relationship between the evolution of the peak intensity and the growth exponent, given the implicit assumption that there is self-similar growth. If the latter is not true, i.e., if the size distribution function changes over time, then it is not possible to replace $N(t)$ in Eq. (6) by a constant times $\langle N(t)\rangle$. The peak intensity must then have a correction factor in it that reflects the changing shape of the intensity profile that results from the changing size distribution function.[39] A changing distribution would imply that it is not possible to extract a meaningful exponent. If one nevertheless interprets the data as if there were self-similar growth, the exponent that is extracted may be either too large or too small, depending on the nature of the evolution of the size distribution. We have assumed that the growth is self-similar, on the basis of profiles at later times, even though we do not actually have profiles at the early times. The fact that the mean sizes are small and the size distributions narrow suggests that any effect due to non-self-similar growth would be negligible in our experiment.

If the detector is not a point detector, errors are made in determining the peak intensity.[39] For example, the use of a slit detector invalidates the relationship of Eq. (7). With a slit detector, there is integration over one direction, reducing the time dependence of the intensity to $I(t)\propto N(t)^{1/2}\propto t^x$. Hence, the measured slope becomes the actual growth exponent, rather than $\frac{1}{2}$ of the slope (the minimum possible) for a true point detector. All finite-size apertures produce a partial integration in both x and y, in principle increasing the growth exponent that is extracted from the measured intensity from its minimum value of $\frac{1}{2}$ of the slope. The greater the integration, the greater the increase. Because profiles become narrower with increasing time, the problem of a finite detector aperture to measure the peak intensity becomes exacerbated at late time. A system growing with a constant growth exponent (straight line on a ln-ln plot) would give a measured intensity on a ln-ln plot that would deviate downward from a straight line. The initial slope of the intensity plot would be close to double the slope of the growth plot, and for sufficient integration, may actually fall below the slope of the growth plot.

One can claim that this is what is, in fact, observed, both by us and by others.[13] There are two problems. One, the break in the ln(intensity)-versus-ln(t) profile is too sharp, and two, at least in our case, the detector does not provide a significant intergration over the data range. In other words, Eq. (7) is applicable as long as self-similar growth is assumed or demonstrated.

How then do we interpret the growth behavior? In theoretical modeling, the difficulty is frequently the existence of a transient before the "true" growth exponent is reached. Is there an analogous transient in experiments? We certainly find the existence of some order as soon as we can begin a measurement. But is it possible that the region up to several hundred seconds, in which we observe a constant rate of increase of the peak intensity, is in fact also a transient, or at least not yet the region in which the calculations find stable behavior and self-similar growth? Is it then further possible that "late-stage growth" can never be reached because of the interference of other phenomena, such as impurity or substrate terrace size effects? These questions are difficult to answer. What is known is that the maximum mean domain sizes that are observed here are much smaller than optimum obtainable sizes (at annealing temperatures near the disordering temperature) and that a growth slowdown occurs long before such sizes are reached.

The results (both the value of the intensity and the time at which the slowdown occurs are temperature dependent) suggest that there is an activated process associated with the initiation of the growth slowdown.[14] The small mean sizes at which the growth slows down suggest that a limited substrate terrace size is probably not the cause of the growth limitation, although this possibility cannot be conclusively excluded. (It is possible that at higher temperatures the barriers at terrace edges are overcome, while they are not at low temperatures.) Second, the temperature dependence of the slowing down suggests that point defects, such as impurities, are not the cause of the slowing down, at least not in the simple manner usually considered. It is difficult to see how defects can be less effective in slowing the growth at higher temperatures than at lower ones unless one again assumes an activated process associated with overcoming the influence of a

point defect.[14] Such a growth slowdown due to diffusive impurities rather than quenched impurities cannot be ruled out but, in fact, calculations appear to show the opposite behavior: at higher temperature a power law is obeyed for a greater time range.[27] We believe that the slowing down is probably related to the nature of domain and island boundaries, akin to the idea of polygonization originally suggested by Lifshitz.[1] There can then be an activation energy associated with overcoming certain types of boundaries that would allow the observed activated process.

If, on the other hand, p is not relevant to ordering, as has been recently suggested,[20,21] polygonization cannot be the cause of slowing down. The only remaining possibilities for slowing growth are impurities and substrate terrace size effects. If impurities are the cause, they would appear to have to be diffusive, which an activation energy for motion, and to have a long-range effect (measurements indicate that only one out of ~ 1000 atoms is an impurity, while the islands on average contain only 25–50 atoms when the slowdown begins; hence one impurity atom affects the growth of many islands). If p is not relevant to the ordering, then one also must wonder how to explain a growth exponent of $x=0.28$ at $\Theta=0.5$ (at the coverages at which there is two-phase coexistence, there is no difficulty). One is left with these choices: (1) the growth observed at early time, before the slowdown, is not "late-stage" growth at all, and the exponent would climb to $x=\frac{1}{2}$ if diffusive-impurity effects did not interfere to, in effect, reduce the exponent; (2) impurities affect the whole growth process, (3) the system is never really at $\Theta=0.5$. One cannot argue against the former to any greater extent than we have already done, namely that we believe that there are very few impurities and that their influence requires an activated process. The second choice requires an explanation of the slowdown in growth if the same impurities are responsible for the growth limitation at all times, and appears unrealistic. Finally, if the system is never really exactly at $\Theta=0.5$, it may find itself locally always in a two-phase coexistence region, where its growth may be governed by the $t^{1/3}$ Lifshitz-Slyozov law. This raises the interesting questions of to what density the $t^{1/3}$ law is valid and how the crossover occurs.

Analysis of the angular profiles of diffracted intensity indicates that dynamical scaling is obeyed in the growth of O on W(110) at several coverages over a certain time regime. At $\Theta=0.5$ the profiles are Gaussians, indicating a Gaussian size distribution function (actually line-length distribution function). The profile measurements correspond to the regime where the growth has slowed. In this regime, dynamic scaling is obeyed. It has not been possible for us to measure profiles at sufficiently early times to test for scaling in the time regime in which we determined the initial growth exponent. We presume that scaling, with a different scaling function, is obeyed in this regime. The data shown in Fig. 8(b) indicate that, as one would expect, dynamic scaling is not well obeyed in the transition region as the system changes from one mechanism to another. At $\Theta=0.25$ the profiles correspond for the most part to the regime for which we extracted a growth exponent of $x=0.28$, but they are more complicated. We have fitted these profiles with a bimodal size distribution. Dynamical scaling is obeyed, but it is difficult to see how a bimodal size distribution can scale. We expect that some other size distribution function can also fit the data. We have extracted mean sizes (lengths) of ordered domains for all coverages and times, but these must be viewed with caution because they are one-dimensional representations of two-dimensional size distributions. Determination of growth exponents from fits to profiles to extract $\langle N \rangle$ versus t give, where it is possible to do so, somewhat lower exponents than the peak intensity. We assume that this is due to the uncertainty in using one-dimensional models to fit one cut through a profile that reflects a two-dimensional size distribution. These aspects are being explored in greater detail.[39]

Finally, we have extracted activation energies for the ordering processes at early times, and have presented arguments on how these activation energies can be interpreted in terms of activation energies for nonequilibrium diffusion. We have shown that a consistent picture of diffusion of O/W(110) arises when the adatom interaction energies for O on W(110) are taken into account. We have shown that studies of ordering can provide the coverage dependence of the activation energy for diffusion on the surface.

ACKNOWLEDGMENTS

This research has been supported by the National Science Foundation (Solid-State Chemistry Program) under Grant No. DMR-86-15089. We thank R. Kariotis for useful discussions.

*Present address: Hong Kong Baptist College, Kowloon, Hong Kong.

†Present address: Department of Physics, Iowa State University of Science and Technology, Ames, IA 50011.

‡Electronic address: Lagally @ WISCPSL.BITNET.

[1] I. M. Lifshitz, Zh. Eksp. Teor. Fiz. **42**, 1354 (1962) [Sov. Phys.—JETP **15**, 939 (1962)].

[2] S. M. Allen and J. W. Cahn, Acta Metall. **21**, 1085 (1979).

[3] K. Binder and D. Stauffer, Phys. Rev. Lett. **33**, 1006 (1974); K. Binder, Phys. Rev. B **15**, 4425 (1977).

[4] P. S. Sahni, D. J. Srolovitz, G. S. Grest, M. P. Anderson, and S. A. Safran, Phys. Rev. B **28**, 2705 (1983).

[5] J. D. Gunton, M. San Miquel, and P. S. Sahni, in *Phase Transitions and Critical Phenomena,* edited by C. Domb and J. L. Lebowitz (Academic, New York, 1983), Vol. 8.

[6] G. F. Mazenko and O. T. Valls, Phys. Rev. B **30**, 6732 (1984); F. C. Zhang, O. T. Valls, and G. F. Mazenko, Phys. Rev. B **31**, 1579 (1985).

[7] A. Sadiq and K. Binder, J. Stat. Phys. **35**, 617 (1984).

[8] I. M. Lifshitz and V. V. Slyozov, J. Chem. Phys. Solids **15**, 35

(1961).
[9]P. S. Sahni and J. D. Gunton, Phys. Rev. Lett. **47**, 1754 (1981).
[10]M. C. Tringides, P. K. Wu, W. Moritz, and M. G. Lagally, Ber. Bunsenges. Phys. Chem. **90**, 277 (1986).
[11]W. Witt and E. Bauer, Ber. Bunsenges. Phys. Chem. **90**, 248 (1986).
[12]M. C. Tringides, P. K. Wu, and M. G. Lagally, Phys. Rev. Lett. **59**, 315 (1987).
[13]J.-K. Zuo and G.-C. Wang, J. Vac. Sci. Technol. A **6**, 649 (1988); J. K. Zuo, G.-C. Wang, and T.-M. Lu, Phys. Rev. Lett. **60**, 1053 (1988).
[14]P. K. Wu, Ph.D. dissertation, University of Wisconsin–Madison, 1987.
[15]M. G. Lagally, T.-M. Lu, and G.-C. Wang, in *Ordering in Two Dimensions,* edited by S. Sinha (Elsevier, New York, 1980).
[16]E. Domany, M. Schick, J. S. Walker, and R. B. Griffiths, Phys. Rev. B **18**, 2209 (1978).
[17]P. Bak, in *Modern Theory of Crystal Growth, I,* Vol. 9 of *Crystals; Growth, Properties, and Applications,* edited by A. A. Chernov and H. Müller-Krumbhaar (Springer-Verlag, Berlin, 1983).
[18]P. A. Rikvold, K. Kaski, and J. D. Gunton, Phys. Rev. B **29**, 6285 (1984).
[19]For lucid reviews, see (a) K. Binder, Ber. Bunsenges. Phys. Chem. **96**, 257 (1986), and (b) J. D. Gunton, in *Kinetics of Interface Reactions,* edited by M. Grunze and H. J. Kreuzer (Springer, New York, 1987).
[20]G. S. Grest, M. P. Anderson, and D. J. Srolovitz, in *Time-Dependent Effects in Disordered Materials,* edited by R. Pynn and T. Riste (Plenum, New York, 1988).
[21](a) H. C. Fogedby and O. G. Mouritsen, Phys. Rev. B **37**, 5962 (1988); O. G. Mouritsen and E. Praestgaard, *ibid.* **38**, 2703 (1988). For recent reviews, see (b) J. D. Gunton, in *Time-Dependent Effects in Disordered Materials,* edited by R. Pynn and T. Riste (Plenum, New York, 1988); (c) J. D. Gunton, J. Vac. Sci. Technol. A **6**, 649 (1988).
[22]M. Tokuyama and K. Kawasaki, Physica A **123**, 386 (1984).
[23]D. A. Huse, Phys. Rev. B **34**, 7845 (1986).
[24]T.-M. Lu and M. G. Lagally, Surf. Sci. **99**, 7845 (1986).
[25]Y. Imry and S.-k. Ma, Phys. Rev. Lett. **35**, 1399 (1975).
[26]J. Villain, J. Phys. (Paris) Lett. **43**, L551 (1982); in *Scaling Phenomena in Disordered Systems,* edited by R. Pynn and A. Skjeltorp (Plenum, New York, 1985).
[27]G. S. Grest and D. J. Srolovitz, Phys. Rev. B **32**, 3014 (1985); D. J. Srolovitz and G. S. Grest, *ibid.* **32**, 3021 (1985).
[28]J. A. Becker, E. J. Becker, and R. G. Brandes, J. Appl. Phys. **32**, 411 (1961).
[29]C. Wang and R. Gomer, in *Proceedings of the 7th International Vacuum Congress and 3rd International Conference on Solid Surfaces,* edited by R. Dobrozemsky, F. Rüdenauer, F. P. Viehbock, and A. Breth (Berger, Vienna, 1977), p. 1155.
[30]T. Engel, H. Niehus, and E. Bauer, Surf. Sci. **52**, 237 (1975).
[31]T.-M. Lu, L. H. Zhao, M. G. Lagally, G.-C. Wang, and J. E. Houston, Surf. Sci. **122**, 519 (1982).
[32]S. A. Safran, Phys. Rev. Lett. **46**, 1581 (1981).
[33](a) R. Kariotis, D. E. Savage, and M. G. Lagally, Surf. Sci. **204**, 491 (1988); (b) R. Kariotis, D. W. Kruger, D. E. Savage, and M. G. Lagally, *ibid.* **205**, 591 (1988).
[34]M. C. Tringides and M. G. Lagally, Surf. Sci. **195**, L159 (1988).
[35]R. Gomer, Surf. Sci. **38**, 373 (1973); J. R. Chen and R. Gomer, *ibid.* **79**, 413 (1979); M. C. Tringides and R. Gomer, *ibid.* **145**, 121 (1984); *ibid.* **155**, 254 (1985).
[36]E. D. Williams, S. C. Cunningham, and W. H. Weinberg, J. Chem. Phys. **68**, 4688 (1978).
[37]R. Butz and H. Wagner, Surf. Sci. **63**, 448 (1977).
[38]M. Bowker and D. A. King, Surf. Sci. **94**, 564 (1980).
[39]R. Kariotis, D. E. Savage, and M. G. Lagally (unpublished).

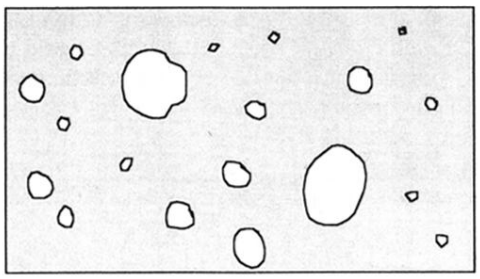

(b) TWO-PHASE SYSTEM

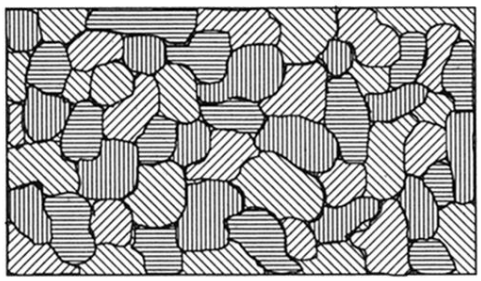

(a) ONE-PHASE SYSTEM

FIG. 3. Schematic diagram of the degree of order at some intermediate time for (a) a one-phase system with ground-state degeneracy $p=4$, and (b) for two phases coexisting with a low concentration of the dense phase. The dilute phase, consisting of monomers at lattice gas sites, is not explicitly shown.